Tractable Robust Drinking Water Pumping to Provide Power Network Voltage Support

Anna Stuhlmacher, Line A. Roald, and Johanna L. Mathieu

Abstract-Drinking water distribution networks can be treated as flexible, controllable assets for power distribution networks (e.g., to provide voltage support) by leveraging the power consumption of water pumps and storage capabilities of water tanks. We formulate an adjustable robust optimization problem to determine the scheduled water distribution network pumping and real-time pump adjustments that ensure that the power and water distribution network constraints are satisfied with respect to uncertain power demand. We extend the monotonicity properties of dissipative flow networks to water distribution networks which requires assumptions on water tank operation. Then, to make the problem tractable, we leverage these properties, along with constraint approximations and an affine pump control policy, to reformulate the problem as an affinely adjustable robust counterpart that solves for the pumping schedule and the parameters of an affine control policy that determines the real-time pump adjustments. Through a case study, we demonstrate that the approach produces robust solutions and is computationally tractable. We also evaluate the impact of restricting water tank operation to enforce monotonicity and find it leads to a significantly restricted feasible region and more conservative solutions.

I. Introduction

The power distribution network (PDN) and the drinking water distribution network (WDN) are coupled critical infrastructure systems. Water pumps in the WDN are loads in the PDN and are capable of shifting their power consumption in time by storing water in elevated water storage tanks. By leveraging the inherent flexibility from the water tanks in the WDN, the WDN can be used as a flexible, controllable asset for the PDN. This work is situated within a growing research area of the integrated optimization of coupled critical infrastructure systems. Potential benefits of integrated optimization include being able to incorporate greater quantities of renewable energy resources, reducing operational and capital costs, and improving system resiliency [1]. However, the problem complexity and dimension significantly increases when incorporating uncertainty sources and nonconvex constraints from multiple networks. Consequently, there is a trade-off in performance between computational tractability and optimality (or feasibility) of the solution.

The goal of this work is to control the pump power consumption in WDNs to manage bus voltages in PDNs with net demand uncertainty (from imperfect forecasts of loads

This work was supported by NSF Graduate Research Fellowship DGE-1256260 and NSF Grant ECCS-1845093. A. Stuhlmacher and J. L. Mathieu are with the Department of Electrical Engineering and Computer Science, University of Michigan, Ann Arbor, MI 48109, USA, akstuhl, jlmath@umich.edu. L. A. Roald is with the Department of Electrical and Computer Engineering, University of Wisconsin-Madison, Madison, WI 53706, USA, roald@wisc.edu.

and intermittent distributed renewables) in a computationally tractable way that can be scaled to large networks and problems with long time horizons. To do so, we formulate the integrated optimization problem as an adjustable robust problem. We leverage monotonicity properties for dissipative flow networks [2], affine control policies, and approximations to reformulate the problem as a computationally tractable affinely adjustable robust counterpart.

There is growing interest in optimization of integrated power-water systems to help support the power network operation. Irrigation systems were used to provide demand response in [3] and the demand response capacity of WDNs is optimized in [4]. Ref. [5] optimizes the electricity consumption flexibility that a group of WDNs can provide to the transmission network. In [6], the WDN consumes surplus energy based on a signal from the PDN. To the best of our knowledge, there are no papers that consider the integrated optimization of PDNs and WDNs considering demand uncertainty besides our previous work [7]. In [7], we formulated a chance-constrained power-water optimization problem considering water and power demand uncertainty and solved it using the scenario approach [8]. One drawback of the scenario approach is that it requires a large amount of data and does not scale well to larger problems. In this paper, we formulate the problem as an Adjustable Robust Optimization (ARO) problem and develop a solution approach to make the problem tractable, resulting in the Affinely Adjustable Robust Counterpart (AARC) that is much more scalable than our chance-constrained approach, but also more conservative.

Leveraging monotonicity properties is a key component in making the robust power-water problem tractable. Monotonicity properties allow us to replace the semi-infinite water network constraints with two sets of deterministic network constraints representing the extreme operating scenarios. By doing so, we provide feasibility guarantees for the entire range of operating scenarios between the two extreme cases. To do this, we leverage the monotonicity properties of dissipative flow networks developed in [2]. This work was extended in [9] for transient gas network modelling and applied in an uncertainty management framework for an integrated gas-power problem in [10]. These papers focus on applying monotonicity properties to gas networks specifically. In this paper, we show how the monotonicity properties of dissipative flow networks apply to WDNs and identify the water tank formulation assumptions required for monotonicity and the impact these assumptions have on the solution space.

The contributions of this work are 1) formulating an ARO

problem to schedule and control water pumping subject to PDN and WDN constraints and power demand uncertainty; 2) deriving water tank operation assumptions to ensure monotonicity properties hold for the WDN; 3) tractably reformulating the AARC using monotonicity properties, convex approximations, and affine control policies; and 4) evaluating the performance of the approach in a case study.

II. ADJUSTABLE ROBUST VOLTAGE SUPPORT PROBLEM

Our goal is to robustly optimize the water pump power consumption subject to the PDN and WDN constraints and power demand uncertainty. Specifically, we seek to determine the scheduled pump power consumption and the parameters of a control policy that determines the real-time pump power consumption adjustments so that the PDN voltage limit constraints are never violated over the scheduling horizon. This formulation can also be interpreted as an optimal power flow problem with water pumps acting as distributed energy resources where the WDN constraints further limit the feasible operation of the water pumps.

In this paper, we do not consider water demand uncertainty. In [7], we simultaneously solved for two separate control policies to adjust pumping as a function of both water and power demand uncertainty. However, the tanks are already designed to hedge against water demand uncertainty [11] and we found that the range of tank flow rate adjustments remains approximately constant over time. Therefore, it is reasonable to assume that a portion of the tank is reserved for responding to water demand uncertainty without explicitly modelling it (similar to how portions of tanks are reserved for emergency fire flow scenarios).

We first formulate the ARO problem as

$$\min_{\mathbf{X}} F(\mathbf{x}, \mathbf{y}(\boldsymbol{\rho}, \mathbf{x})) \qquad (ARO)$$
s.t. $\forall \boldsymbol{\rho} \in \mathcal{U}, \exists \mathbf{y},$

$$\nu_1(\mathbf{x}, \mathbf{y}(\boldsymbol{\rho}, \mathbf{x}), \boldsymbol{\rho}) \leq 0,$$

$$\nu_2(\mathbf{x}, \mathbf{y}(\boldsymbol{\rho}, \mathbf{x}), \boldsymbol{\rho}) \leq 0,$$

$$\nu_3(\mathbf{x}, \mathbf{y}(\boldsymbol{\rho}, \mathbf{x}), \boldsymbol{\rho}) \leq 0.$$

ARO is a multi-stage robust optimization problem containing random variable ρ in the uncertainty set \mathcal{U} , the operational ('here-and-now') variable x which is feasible for all uncertainty realizations within the uncertainty set \mathcal{U} , and the adjustable ('wait-and-see') variable $y(\rho, x)$ which can be decided given a specific uncertainty realization [12]. In our problem, the uncertainty ρ is the power demand at every bus and phase, the operational variable x includes the scheduled pump power consumption, and the adjustable variable $y(\rho)$ includes the pump power consumption adjustment which is a function of the power demand forecast error. The functions $\nu_1(\cdot)$ and $\nu_3(\cdot)$ contain the quasi-steady state PDN and WDN constraints (i.e., steady state operation for every time step of duration ΔT within the scheduling horizon \mathcal{T}). Function $\nu_2(\cdot)$ links the WDN and PDN; specifically, it contains the real-time pump adjustments which impact both the power flow and water flow. The cost function $F(\cdot)$ includes the cost of the pump schedule and real-time adjustments.

ARO is less conservative than classic robust optimization problems because decisions can be updated in real-time [12]. Unlike a chance-constrained optimization problem in which the constraints must be satisfied at a specified probability, ARO constraints must be satisfied for all uncertainty realizations within the uncertainty set.

We next model the PDN $\nu_1(\cdot)$ and the pump adjustments $\nu_2(\cdot)$ which ensure that the minimum and maximum voltage limits are satisfied. Then, we present the basic form of the AARC. In the next section, we derive the WDN constraints $\nu_3(\cdot)$ that limit the pump power consumption and present the full AARC.

A. Power Distribution Network Modelling

We first define $\nu_1(\cdot)$. We consider an unbalanced, radial PDN that includes a set of buses K and phases Φ to which the uncontrollable net loads (i.e., actual load minus distributed generation) and the controllable pumps are connected. To facilitate the derivation of the robust counterpart, we use a linearized power flow model, specifically, the 3-phase unbalanced power flow model from [13] also referred to as Lin3DistFlow. We note that other linearized unbalanced power flow models, e.g., [14], could also be used. It is also possible that more accurate nonlinear 3-phase unbalanced power flow models could be used; however, this would complicate our formulation and, since our focus is on the WDN, we leave this to future work. The power flow equations are

$$oldsymbol{P}_k^t = oldsymbol{
ho}_k^t + oldsymbol{p}_e^t + \sum_{n \in \mathcal{I}_k} oldsymbol{P}_n^t \qquad \quad orall \ k \in \mathcal{K}, t \in \mathcal{T}, \quad (1)$$
 $oldsymbol{Q}_k^t = oldsymbol{\zeta}_k^t + \eta_e oldsymbol{p}_e^t + \sum_{n \in \mathcal{I}_k} oldsymbol{Q}_n^t \qquad \quad orall \ k \in \mathcal{K}, t \in \mathcal{T}, \quad (2)$

$$Q_k^t = \zeta_k^t + \eta_e p_e^t + \sum_{n \in \mathcal{T}_k} Q_n^t \qquad \forall k \in \mathcal{K}, t \in \mathcal{T}, \quad (2)$$

$$\boldsymbol{Y}_{k}^{t} = \boldsymbol{Y}_{n}^{t} - \boldsymbol{M}_{kn} \boldsymbol{P}_{n}^{t} - \boldsymbol{N}_{kn} \boldsymbol{Q}_{n}^{t}, \quad \forall \ k \in \mathcal{K}, t \in \mathcal{T}, \quad (3)$$

where (1) and (2) represent the active and reactive power balance at each node k and (3) represents the voltage drop across the line. The parameter \boldsymbol{Y}_k^t is the 3-phase voltage magnitude squared at bus k and time t, \boldsymbol{P}_k^t and \boldsymbol{Q}_k^t are the 3phase real and reactive power flows entering bus $k,\, \boldsymbol{M}_{kn}$ and N_{kn} are the parameter matrices for line kn, ρ_k^t and ζ_k^t are the 3-phase real and reactive uncontrollable power demand at bus k, p_e^t is the 3-phase power consumption of pump e (where the pumps are modelled as balanced 3-phase constant power loads with constant power factor), and \mathcal{I}_k is the set of buses directly downstream bus k. The pump power consumption p_e^t is zero if there are no pumps connected to bus k. The parameter η_e is the real-to-reactive power consumption ratio of pump e. We bound the voltages at all buses, phases, and time periods by V and \overline{V} , i.e.,

$$\underline{\boldsymbol{V}}^2 \le \boldsymbol{Y}_k^t \le \overline{\boldsymbol{V}}^2 \quad \forall \, k \in \mathcal{K}, t \in \mathcal{T}.$$
 (4)

B. Real-Time Pump Adjustments Responding to Uncertainty

We next define $\nu_2(\cdot)$. The source of uncertainty is the realtime uncontrollable power demand vector $\boldsymbol{\rho}^t := \bar{\boldsymbol{\rho}}^t + \Delta \boldsymbol{\rho}^t$, which is composed of the forecasted power demand $\bar{\rho}^t$ (a known parameter) and the uncertain but bounded forecast error $\Delta \rho^t := [\Delta \rho_{k,\phi}^t]_{k \in \mathcal{K}, \phi \in \Phi}$. We assume that water supply pumps in the WDN are adjusted according to a decision rule that is a function of $\Delta \rho^t$. Specifically, we define an affine pump power control policy and solve for the policy parameters as 'here and now' decisions. Using an affine policy allows us to represent the response of the system without needing to resolve the problem for each uncertainty realization. This makes it easier for water utilities to implement the control policy in real-time. However, the use of an affine policy also restricts the feasible space, meaning that our solutions may be conservative. The control policy allows us to write the adjustable power variables (e.g., voltage magnitude squared) as affine functions of the random variables. The real-time single-phase pump power consumption is

$$p_e^t = p_{\text{nom},e}^t + C_e^t \Delta \rho^t \quad \forall e \in \mathcal{P}, t \in \mathcal{T},$$
 (5)

where $p_{\text{nom},e}^t$ is the scheduled single-phase power consumption of pump e at time t, C_e^t is a control policy parameter row vector that determines the single-phase adjustment of pump e at time t as a function of $\Delta \rho^t$, and \mathcal{P} is the set of pumps. To implement this, the water system operator needs real-time data on the power demand forecast error at each bus and phase. While this may be unrealistic at the present time, this formulation and results point to the value of real-time pump adjustments; future work will explore whether this value outweighs the costs of the infrastructure needed to support it.

We additionally assume that the cost of the real-time pump adjustments is a function of the adjustment range and define $R_{\rm up}$ and $R_{\rm dn}$ as the largest increase and decrease in pump power, i.e.,

$$-R_{\mathrm{dn},e}^{t} \leq 3C_{e}^{t} \Delta \rho^{t} \leq R_{\mathrm{up},e}^{t} \quad \forall e \in \mathcal{P}, t \in \mathcal{T},$$

$$R_{\mathrm{up},e}^{t}, R_{\mathrm{dn},e}^{t} \geq 0 \quad \forall e \in \mathcal{P}, t \in \mathcal{T},$$
(6a)

where we multiply the single-phase pump power adjustment by 3 to get the total 3-phase power demand.

C. Basic Form of the AARC

The cost function, which is now only a function of the operational variables, is

$$F(\mathbf{x}) = \sum_{e \in \mathcal{P}, t \in \mathcal{T}} 3\pi_e^t p_{\text{nom}, e}^t + \pi_{\text{vs}, e}^t (R_{\text{up}, e}^t + R_{\text{dn}, e}^t), \quad (7)$$

where π_e^t is the cost of electricity for the pump e at time t and $\pi_{vs,e}^t$ is the cost associated with the real-time adjustment range. The operational decision variables in the PDN constraints include p_{nom} , C, R_{dn} , and R_{up} . The adjustable decision variables in the PDN constraints include the voltage magnitude squared Y and are linear in the random variables $\Delta \rho$ and so we can tractably reformulate $\nu_1(\cdot)$, i.e., the power flow equations and constraints (1)-(4), and $\nu_2(\cdot)$, i.e., the affine control policy and associated constraints (5)-(6b), given the uncertainty set \mathcal{U} . We use explicit maximization [15] to derive the robust counterpart of $\nu_1(\cdot)$ and $\nu_2(\cdot)$. Assuming we can also obtain the robust

counterpart of the WDN constraints $\nu_3(\cdot)$, we can write the basic form of the AARC as

$$\min_{\mathbf{X}} \quad (7) \qquad (AARC)$$
s.t. $\omega_1(\mathbf{x}) \le 0$, $\omega_2(\mathbf{x}) \le 0$, $\omega_3(\mathbf{x}) \le 0$,

where $\omega_1(\mathbf{x}) \leq 0$, $\omega_2(\mathbf{x}) \leq 0$ represent the robust reformulation of (1)-(6b) and $\omega_3(\mathbf{x}) \leq 0$ is the robust reformulation of the WDN constraints, which we derive in the next section.

III. INCORPORATING WDN CONSTRAINTS

We need to ensure that the WDN constraints are satisfied for any real-time pump power consumption determined by the affine control policy (5). As a result, the flow rates, hydraulic heads, and tank levels are adjustable variables. In this section, we present the WDN constraints that are included in the ARO, show how the monotonicity properties in [2] apply to the WDN which allows us to tractably reformulate the WDN constraints, and describe the tank formulation assumptions required to ensure monotonicity.

A. Water Distribution Network Modelling

The WDN can be represented as a directed graph $G=(\mathcal{N},\mathcal{E}),$ where \mathcal{N} is the set of nodes and \mathcal{E} is the set of edges. The incidence matrix A describes connections between the nodes and edges where all edges are assigned an arbitrary direction. Set \mathcal{N} is composed of disjoint subsets of junctions $\mathcal{J},$ reservoirs $\mathcal{R},$ and elevated storage tanks $\mathcal{S},$ i.e., $\mathcal{N}=\mathcal{J}\cup\mathcal{R}\cup\mathcal{S}.$ The edges are bi-directional pipes that connect nodes. A pipe may contain at most one pump, i.e., $\mathcal{P}\subseteq\mathcal{E}.$ The WDN at time t can be characterized by the hydraulic heads $\mathbf{H}^t:=[H_j^t]_{\forall j\in\mathcal{N}}$ at all nodes and the volumetric flow rates $\mathbf{x}^t:=[x_{ij}^t]_{\forall (i,j)\in\mathcal{E}}$ through all pipes going from node i to node j.

WDNs are dissipative flow networks [2] and are governed by the following equations

$$\sum_{i:(i,j)\in\mathcal{E}} x_{ij}^t + d_j^t = 0 \quad \forall j \in \mathcal{N}, t \in \mathcal{T},$$
 (8)

$$x_{ij}^{t} = -x_{ji}^{t} \quad \forall (i,j) \in \mathcal{E}, t \in \mathcal{T},$$
 (9)

$$H_i^t - H_j^t = f_{ij}(x_{ij}^t) \quad \forall (i,j) \in \mathcal{E}, t \in \mathcal{T}, \tag{10}$$

where d_j^t is the injection of water at node j and time t, where positive values indicate an injection into the network and negative values indicate a withdrawal from the network. Customer water demands at junctions are assumed to be known and non-positive. In (8), the conservation of water at each node is enforced. Since the flow along pipes can be bi-directional, (9) enforces skew symmetry along pipe ij at time t. The head loss equation (10) describes the relationship between hydraulic head at nodes and flow rate over a pipe or pump connecting them. The head loss function $f_{ij}(\cdot)$ is continuous and increasing with respect to flow rate x_{ij}^t . The

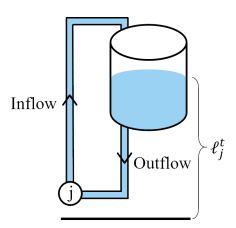


Fig. 1. Water storage tank diagram.

pipe head loss function is commonly modelled using the Darcy-Weisbach formulation [16]

$$f_{ij}(x_{ij}^t) = k_{ij}|x_{ij}^t|x_{ij}^t \quad \forall (i,j) \in \mathcal{E} \setminus \mathcal{P}, t \in \mathcal{T},$$

where parameter k_{ij} is the resistance coefficient of pipe ij. The pump head is typically modelled as a quadratic function

$$f_{ij}(x_{ij}^t) = -(m_{ij}^0 - m_{ij}^1(x_{ij}^t)^2) \quad \forall (i,j) \in \mathcal{P}, t \in \mathcal{T},$$

where m^0_{ij} and m^1_{ij} are parameters. Additional constraints needed to model the WDN are given next by component

1) Junctions: The hydraulic head, which is composed of the elevation head and the pressure head, is bounded at all nodes

$$\underline{\boldsymbol{H}} \le \boldsymbol{H}^t \le \overline{\boldsymbol{H}} \quad \forall \, t \in \mathcal{T}, \tag{11}$$

where H and \overline{H} are the minimum and maximum heads.

2) Tanks: Tanks are connected to a single node in the WDN, where we separately model the tank's inflow and outflow from the node (see Fig. 1). The tank inlet is typically located at the top of the tank. The tank constraints are

$$\ell_j^{t=|\mathcal{T}|} \ge \ell_j^{t=0} \quad \forall \ j \in \mathcal{S},$$
 (12a)

$$\ell_j^t = \ell_j^{t-1} + \frac{\Delta T}{\gamma_j} A_j \boldsymbol{x}^t \quad \forall \ j \in \mathcal{S}, t \in \mathcal{T},$$
 (12b)

$$\underline{\ell_j} \le \ell_j^t \le \overline{\ell_j} \quad \forall \ j \in \mathcal{S}, t \in \mathcal{T}, \tag{12c}$$

$$g_j(\boldsymbol{x}^t, \ell_j^t) \le 0 \quad \forall \ j \in \mathcal{S}, t \in \mathcal{T},$$
 (12d)

where ℓ_i^t is the water level (including elevation) at tank j and time t, γ_i is the cross-sectional area of the tank, and A_i is row j in the incidence matrix A. In (12a), we ensure that the tanks are not depleted over the scheduling horizon by setting the final tank level to be greater than or equal to the initial tank level. The water level ℓ_i^t is defined in (12b) and bounded in (12c) to reflect the physical volume of the tank. Function $g_i(\cdot)$ in (12d) contains tank head constraints that depend upon our tank formulation which we will describe in more detail in Section III-B.1. The tank head determines whether the tank is storing or supplying water to the network. When the tank in Fig. 1 has no valves or pumps, it stores water if the tank head is greater than the head associated with the maximum tank level and supplies water if the tank head is equal to the head associated with the tank level. In order for WDN monotonicity to hold, we need to make certain assumptions about tank equipment and operation, which will be discussed in Section III-B.1.

3) Reservoirs: Reservoirs are modelled as infinite sources and the head is fixed

$$H_j^t = \overline{h}_j \quad \forall j \in \mathcal{R}, t \in \mathcal{T}.$$
 (13)

4) Pipes and Pumps: Pipes without pumps can have positive or negative flows. Pumps have bounded unidirectional flows, i.e.,

$$0 \le \underline{x}_{ij} \le x_{ij}^t \le \overline{x}_{ij} \quad \forall (i,j) \in \mathcal{P}, t \in \mathcal{T}. \tag{14}$$

We consider fixed speed supply pumps whose on/off status is unchanged throughout the scheduling horizon. The singlephase pump power consumption is

$$p_e^t = b(x_{ij}^t) \ \forall e = (i, j) \in \mathcal{P}, t \in \mathcal{T}, \tag{15}$$

where function $b(\cdot)$ calculates the power consumed by the pump and assigns a third of the total pump power consumption to each phase. For fixed speed pumps, this function is traditionally modelled as a cubic [5], [6], quadratic [3], or linear function [4], [17], [18] of flow rate or head gain. Here, we assume a linear function of flow rate

$$p_e^t = h_{ij}^0 + h_{ij}^1 x_{ij}^t \quad \forall e = (i, j) \in \mathcal{P}, t \in \mathcal{T},$$

where h_{ij}^0 and h_{ij}^1 are parameters. Including these WDN constraints within the problem results in a semi-infinite program since (8)-(15) represent infinitely many constraints and adjustable variables x_{ij}^t , ℓ_i^t , and H_i^t associated with every possible realization of the power demand forecast error in the uncertainty set. However, we can leverage monotonicity properties to tractably reformulate the WDN constraints.

B. Monotonicity of WDNs

Next, we establish that the hydraulic heads H^t and tank levels ℓ^t are monotonic functions of the reservoir water injection and controllable pump power consumption. This allows us to replace the semi-infinite water flow equations with two sets of deterministic constraints that consider only the minimum and maximum water injections.

In order to formulate the equivalent deterministic water constraints, we must first prove the uniqueness of the water flow solution given the water injections. If there exists a unique solution, we can write the adjustable variables as functions of the injections and evaluate the relationship between the water injections and the adjustable variables. Next, we need to prove that the adjustable variables are monotonic functions of the water injections (which vary based on the uncertain power demand in the PDN). We build our analysis on the monotonicity proofs for dissipative flow networks in [2], [9]; however, there are several key differences. The WDN requires additional formulation assumptions to ensure monotonicity because of the additional adjustable variables in the WDN (i.e., the tank levels) and the external constraints on tank head. For example, we must ensure that the tank level is a monotonic function of the reservoir water injections since the tank level is a bounded adjustable variable.

1) Network Assumptions: We need to make the following three assumptions for the monotonicity properties to apply to the WDN. Note that the superscript t is dropped in this subsection for brevity.

Assumption 1: The head loss function $f_{ij}(x_{ij}) \, \forall \, (i,j) \in \mathcal{E}$ and pump power consumption are increasing in flow rate. This assumption is in [2]. In the WDN, this assumption holds for head loss in pipes and pumps whose on/off status is fixed before the scheduling horizon. The pipe head loss function is commonly modelled using the experimental Hazen-Williams equation or theoretical Darcy-Weisbach equation, and in both equations, the head loss is increasing with flow rate. We assume the pump power consumption is increasing in flow rate, which follows general power characteristic curves [19].

rate, which follows general power characteristic curves [19]. Assumption 2: If $d_j{}^{(1)} \leq d_j{}^{(2)} \ \forall j \in \mathcal{R}$ and $d_j{}^{(1)} = d_j{}^{(2)} \ \forall j \in \mathcal{J}$, then $d_j{}^{(1)} \geq d_j{}^{(2)} \ \forall j \in \mathcal{S}$. Given an increase in reservoir water injections, we need to assume all tank injections decrease. This assumption is always true for a single tank network since water injections must sum to zero. However, for this to be true in a multiple tank case, we need an additional constraint that limits tank injection adjustments to all be in the same direction. This limits the possible feasible WDN solutions.

Assumption 3: The tank head is not strictly dependent on the tank level. If the tank head *is* strictly dependent on the tank level, an increase in reservoir water injection would cause an increase in tank level and, consequently, tank head. As a result, the junction heads surrounding the tank may not be monotonically decreasing. We next consider two tank formulations that satisfy this assumption and derive the associated head constraints (12d). In both formulations, the tank water injections become decision variables.

Tank Formulation 1. We assume that a valve is connected to the tank's outlet pipe so that we can control the outlet flow rate/head, similar to [11], [17]. In this setup, the tank heads must satisfy additional inequality constraints if the tank is storing or supplying water. The constraints included in (12d) in this formulation are

$$-M\alpha_{j} \leq d_{j} \leq M\alpha_{j} \quad \forall \ j \in \mathcal{S}, \quad \text{(16a)}$$

$$-M\beta_{j} \leq d_{j} \leq M(1-\beta_{j}) \quad \forall \ j \in \mathcal{S}, \quad \text{(16b)}$$

$$-M(1-\alpha_{j}) \leq \widetilde{H}_{j} - H_{j} \leq M(1-\alpha_{j}) \quad \forall \ j \in \mathcal{S}, \quad \text{(16c)}$$

$$\overline{\ell}_{j} - M(1-\beta_{j}) \leq \widetilde{H}_{j} \leq \ell_{j} + M\beta_{j} \quad \forall \ j \in \mathcal{S}, \quad \text{(16d)}$$

$$\alpha_{j}, \beta_{j} \in \{0, 1\}, \quad \quad \text{(16e)}$$

where M>0 is a large number, α_j is a binary variable that determines whether tank j is connected, and β_j is a binary variable that determines whether tank j is filling. Constraint (16a) sets the tank water injection to zero if the tank is not connected. In (16b), the tank is filling or emptying given a positive or negative tank injection. In (16c), \widetilde{H}_j is an auxiliary head variable. If the tank is connected, then the head at the tank node is equal to \widetilde{H}_j ; otherwise the constraint holds trivially. In (16d), if tank j is emptying, then $H_j \leq \ell_j$. If tank j is filling, then $H_j \geq \overline{\ell}_j$.

Tank Formulation 2. The tank level has no impact on the tank head, similar to [3], [20]. For this assumption to be feasible, the tank's inlet and outlet pipes need a booster pump and a valve, respectively. This formulation provides the most flexibility in the water flow solution. No additional head constraints are needed in (12d). A drawback to this formulation is that the tank is no longer passive and the booster pump consumes energy.

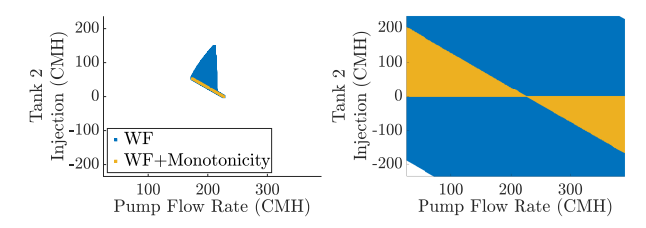


Fig. 2. The feasible water flow solutions for tank formulation 1 (Left) and tank formulation 2 (Right) are shown in blue with an overlaid orange area indicating the feasible water flow solutions when enforcing monotonicity.

In Fig. 2, we demonstrate the feasible water flow solutions for tank formulations 1 and 2 using the coupled PDN-WDN presented in Section V. For combinations of pump and tank injections, we check if there exists a water flow solution given the mixed-integer nonconvex water flow constraints. Tank formulation 1 is less flexible than tank formulation 2 because the head and water level of the tanks limit when the tank can store or supply water. Additionally, Fig. 2 also shows the feasible solutions that satisfy monotonicity (i.e., the addition of Assumption 2 since Assumptions 1 and 3 are already met). For this case study, we found that the feasible range of pump flow rates is the same regardless of the monotonicity constraint; however, the feasible combinations of tank injections are significantly limited. However, tank injection combinations that are not feasible under monotonicity are cases in which the tanks are counteracting each other, and so may correspond to more expensive (i.e., suboptimal) operating points. In our case study, we use tank formulation 2 since the WDN has more flexibility and can provide more voltage support. Our current formulation does not consider the power consumption of the tank's booster pump which we plan to model in future work.

- 2) Existence and Uniqueness: Existence and uniqueness of WDNs has been proven many times in the literature. Given the water injections at all nodes, if the water flow equations (8)-(10) are feasible and the head loss equation is monotonically increasing in flow, then there exists a unique solution to the water flow equations [21], [22].
- 3) Monotonicity of Head with Water Injections: We use the Aquarius Theorem from [2] to show monotonicity of the junction heads given reservoir water injections. The Aquarius Theorem is summarized for comprehensiveness:

Aquarius Theorem [2]: Consider two sets of flow rates $\boldsymbol{x}^{(1)}$ and $\boldsymbol{x}^{(2)}$ that satisfy (8) for injection vectors $\boldsymbol{d}^{(1)}$ and $\boldsymbol{d}^{(2)}$. Let $\mathcal{B} \subset \mathcal{N}$. If $d_i^{(1)} \geq d_i^{(2)} \, \forall \, i \in \mathcal{B}$, then for every $i \in \mathcal{B}$, there exists a nonintersecting path $i_1,...,i_K$, where $i_1 \in \mathcal{N} \setminus \mathcal{B}$ and $i_K = i$ such that $x_{i_k i_{k+1}}^{(1)} \leq x_{i_k i_{k+1}}^{(2)} \, \forall \, k = 1,...,K-1$. The Aquarius Theorem states that given an ordered water

The Aquarius Theorem states that given an ordered water injection, there is a path of ordered water flows. Therefore, we can make the following statement:

Proposition 1: Consider the solutions $(\boldsymbol{x}^{(1)}, \boldsymbol{H}^{(1)})$ and $(\boldsymbol{x}^{(2)}, \boldsymbol{H}^{(2)})$ satisfying the conservation of water equation (8) and the head loss equation (10) for water injection vectors $\boldsymbol{d}^{(1)}$ and $\boldsymbol{d}^{(2)}$. If $d_i^{(1)} \leq d_i^{(2)}$ for all $i \in \mathcal{R}$, then $H_j^{(1)} \geq H_i^{(2)}$ for every node $j \in \mathcal{N} \setminus \mathcal{R}$.

Proof: We define sets $\mathcal{B} = \{\mathcal{S} \cup \mathcal{J}\}$ and $\mathcal{N} \setminus \mathcal{B} = \mathcal{R}$. Given Assumption 2, we know that $d_j^{(1)} \geq d_j^{(2)} \, \forall \, j \in \mathcal{S}$

since $d_i^{(1)} \leq d_i^{(2)} \, \forall i \in \mathcal{R}$. Using the Aquarius Theorem, we know there is a nonintersecting path between every node in $\mathcal B$ to a node in $\mathcal R$ that has an ordered flow rate since $d_i^{(1)} \geq d_i^{(2)}$ for all $i \in \mathcal{B}$ (i.e., $d_i^{(1)} \geq d_i^{(2)}$ for all $i \in \mathcal{S}$ and $d_i^{(1)} = d_i^{(2)}$ for all $i \in \mathcal{J}$). We calculate the cumulative head loss along the nonintersecting path $i_1, ... i_{K-1}$ defined in the Aquarius Theorem from $j \in \mathcal{R}$ to $i \in \mathcal{B}$, i.e.,

$$H_j - H_i = \sum_{k=1}^{K-1} f_{i_k i_{k+1}}(x_{i_k i_{k+1}}) \quad \forall i \in \mathcal{B}, \exists j \in \mathcal{R}.$$

We know that $H_j^{(1)} = H_j^{(2)}$ for all $j \in \mathcal{R}$ since reservoirs are treated as infinite sources with fixed pressure heads. Since $d_i^{(1)} \geq d_i^{(2)}$, through the Aquarius Theorem, we know that $x_{i_k i_{k+1}}^{(1)} \leq x_{i_k i_{k+1}}^{(2)} \, orall \, k = 1,..,K-1$ along the path and

$$H_i^{(1)} = H_j^{(1)} - \sum_{k=1}^{K-1} f_{i_k i_{k+1}}(x_{i_k i_{k+1}}^{(1)}) \ge H_j^{(2)} - \sum_{k=1}^{K-1} f_{i_k i_{k+1}}(x_{i_k i_{k+1}}^{(2)}) = H_i^{(2)}.$$

Therefore, if $d_i^{(1)} \leq d_i^{(2)}$ for all $i \in \mathcal{R}$ then $H_j^{(1)} \geq H_j^{(2)}$ for every node $j \in \mathcal{N} \setminus \mathcal{R}$. Conversely, if $d_i^{(1)} \geq d_i^{(2)}$ for all $i \in \mathcal{R}$ then $H_j^{(1)} \leq H_j^{(2)}$ for every node $j \in \mathcal{N} \setminus \mathcal{R}$.

This implies that the maximum head occurs at the minimum reservoir water injection. Conversely, the minimum head occurs at the maximum reservoir water injection.

4) Monotonicity of Tank Level with Water Injections:

Proposition 2: Consider the solutions $(x^{(1)}, H^{(1)})$ and $(x^{(2)}, H^{(2)})$ satisfying the conservation of water equation (8) and the head loss equation (10) for water injection vectors $\mathbf{d}^{(1)}$ and $\mathbf{d}^{(2)}$. If $d_i^{(1)} \geq d_i^{(2)}$ for all $i \in \mathcal{R}$, then $\ell_j^{(1)} \geq \ell_j^{(2)}$ for every tank $j \in \mathcal{S}$.

Proof: An increase in reservoir injection causes a decrease in tank injection (Assumption 2). Since the tank level increases given a decreasing tank injection (12b), we know that the tank level increases with increasing reservoir injection.

We are able to extend the monotonicity properties in Propositions 1 and 2 to the pump power consumption since we are considering supply pumps that are directly downstream of reservoirs. For these pumps, an increase in the reservoir water injection is directly related to an increase in water flow through the pump. Since the power consumption increases with flow (Assumption 1), we know that the power consumption increases with increasing reservoir injection.

Therefore $\nu_3(\cdot)$ in the ARO can be replaced with the two extreme sets of pump power consumption and the scheduled pump power consumption

$$\Gamma_{\text{scheduled}}(\boldsymbol{p}_{\text{nom}}) \le 0,$$
 (17a)

$$\Gamma_{\text{extreme}}(\overline{p}) \le 0,$$
 (17b)

$$\Gamma_{\text{extreme}}(\boldsymbol{p}) \le 0,$$
 (17c)

where $\Gamma_{scheduled}(\cdot)$ is the set of WDN equations (8)-(15) for the scheduled operation and $\Gamma_{\text{extreme}}(\cdot)$ is the set of WDN

equations (8)-(11), (12b)-(15) for the extreme cases. We use an overbar and underbar to denote the sets of WDN variables for the maximum and minimum extreme cases, e.g., \overline{H} and H. The maximum and minimum pump power consumptions are defined by the scheduled pump power consumption, $R_{\rm up}$,

$$\overline{p}_{e}^{t} = p_{\text{nom},e}^{t} + (1/3)R_{\text{up},e}^{t} \qquad \forall e \in \mathcal{P}, t \in \mathcal{T}, \quad (18a)$$

$$\underline{p}_{e}^{t} = p_{\text{nom},e}^{t} - (1/3)R_{\text{dn},e}^{t} \qquad \forall e \in \mathcal{P}, t \in \mathcal{T}, \quad (18b)$$

$$\underline{p}_{e}^{t} = p_{\text{nom},e}^{t} - (1/3)R_{\text{dn},e}^{t} \qquad \forall e \in \mathcal{P}, t \in \mathcal{T},.$$
 (18b)

Since the pumps are balanced 3-phase loads, we divide the magnitude of the largest pump power adjustments by 3 to get the single-phase pump power consumption. Additionally, we enforce Assumption 2 in the extreme cases by including

$$\overline{d}_{j}^{t} \leq d_{\text{nom},j}^{t} \quad \forall j \in \mathcal{S}, t \in \mathcal{T},$$
 (19a)

$$\underline{d}_{j}^{t} \ge d_{\text{nom},j}^{t} \quad \forall j \in \mathcal{S}, t \in \mathcal{T}, \tag{19b}$$

in (17b) and (17c), respectively, where $d_{\text{nom},j}^t$ is the scheduled reservoir water injection and \overline{d}_{j}^{t} , \underline{d}_{j}^{t} corresponds to the water injections in the extreme scenarios.

C. Full AARC

Finally, we replace the general expression of the robust reformulation of the WDN constraints $\omega_3(\mathbf{x})$ with three sets of deterministic constraints to obtain the full AARC

$$\begin{aligned} & \underset{\mathbf{X}}{\min} & (7) & (\mathbf{AARC}) \\ & \text{s.t.} & & \omega_1(\mathbf{x}) \leq 0, \\ & & & \omega_2(\mathbf{x}) \leq 0, \\ & & & (17), (18), \end{aligned}$$

where $\mathbf{x} = \{p_{\text{nom}}, \underline{p}, \overline{p}, R_{\text{up}}, R_{\text{dn}}, C, H, \ell, x, \underline{H}, \underline{\ell}, \underline{x}, \overline{H}, \underline{\ell}, \underline{x}, \underline{H}, \underline{\ell}, \underline{x}, \overline{H}, \underline{\ell}, \underline{x}, \overline{H}, \underline{\ell}, \underline{x}, \underline{H}, \underline{\ell}, \underline{x}, \overline{H}, \underline{\ell}, \underline{x}, \underline{H}, \underline{\ell}, \underline{x}, \overline{H}, \underline{\ell}, \underline{x}, \underline{H}, \underline{\ell}, \underline{\ell}, \underline{x}, \underline{H}, \underline{\ell}, \underline{\ell}, \underline{x}, \underline{H}, \underline{\ell}, \underline{\ell}$

IV. WDN APPROXIMATIONS

Additionally, we approximate several of the deterministic WDN constraints in the AARC to convexify the problem and reduce computation time. Importantly, these approximations are not necessary to guarantee robustness; the monotonicity properties used in Section III guarantee robustness for the nonconvex WDN constraints.

The head loss equations for pipes and pumps (10) are nonconvex. We replace the head loss function $f_{ij}(x_{ij}^t)$ for pipes with a quasi-convex hull of the Darcy-Weisbach formulation so we can model pipes with bi-directional flow [3]

$$H_{i}^{t} - H_{j}^{t} \leq (2\sqrt{2} - 2)k_{ij}\overline{x}_{ij}x_{ij}^{t} + (3 - 2\sqrt{2})k_{ij}\overline{x}_{ij}^{2},$$

$$H_{i}^{t} - H_{j}^{t} \geq (2\sqrt{2} - 2)k_{ij}|\underline{x}_{ij}|x_{ij}^{t} - (3 - 2\sqrt{2})k_{ij}\underline{x}_{ij}^{2},$$

$$H_{i}^{t} - H_{j}^{t} \geq 2k_{ij}\overline{x}_{ij}x_{ij}^{t} - k_{ij}\overline{x}_{ij}^{2},$$

$$H_{i}^{t} - H_{j}^{t} \leq 2k_{ij}|\underline{x}_{ij}|x_{ij}^{t} + k_{ij}\underline{x}_{ij}^{2},$$
(20)

 $\forall (i,j) \in \mathcal{E} \setminus \mathcal{P}, t \in \mathcal{T}$. Parameters \underline{x}_{ij} and \overline{x}_{ij} are lower and upper bounds on pipe ij's flow rate. We under-approximate the pump head gain as a linear function

$$H_i^t - H_i^t = m_{ij}^3 x_{ij}^t + m_{ij}^2 \quad \forall (i,j) \in \mathcal{P}, t \in \mathcal{T},$$
 (21)

where m_{ij}^3 and m_{ij}^2 are parameters. Therefore, the convexified (AARC) replaces (10) in (17) with (20)-(21).

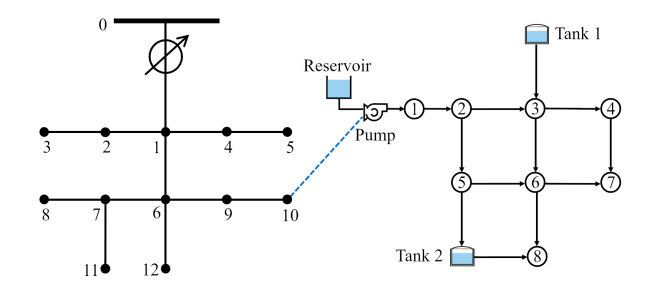


Fig. 3. Coupled PDN (left) and WDN (right). The blue dashed line indicates where the water supply pump is connected to the PDN.

V. CASE STUDY

In our case study, we use a coupled PDN and WDN shown in Fig. 3. We first describe the case study set up and then present our case study results.

A. Set Up

The WDN is a test network (NET1) included with EPANET, a free WDN modelling and simulation software program developed by the U.S. Environmental Protection Agency [23]. We pull the network data from the EPANET input file and make the following modifications. We added an additional tank (tank 2) in order to evaluate a case study that requires the tank injection monotonicity constraints (19). We reduced the volume of the first tank so that the total water storage capacity remains the same. The updated tank data is $\gamma_j=94.53~\text{m}^2,~\ell_j^0=327.06~\text{m},~\ell_j=319.56~\text{m},~\text{and}~\overline{\ell_j}=334.56~\text{m}$ for tank 1 and $\gamma_j=94.54~\text{m}^2,~\ell_j^0=339.02~\text{m},~\ell_j=331.52~\text{m},~\text{and}~\overline{\ell_j}=346.52~\text{m}$ for tank 2. The minimum head limit at each junction is equal to the elevation plus a minimum pressure head of 20 m. The pump performance coefficients are $h_{ij}^1=1.09~\text{kW/CMH},~h_{ij}^0=-22.88~\text{kW},~m_{ij}^1=-9.08\times10^{-2}~\text{m/CMH},~\text{and}~m_{ij}^0=103.73~\text{m}$ with a minimum and maximum flow rate of $\underline{x}_{ij}=25~\text{CMH}$ and $\overline{x}_{ij}=390~\text{CMH},~\text{respectively}.$

For the three-phase unbalanced PDN, we use the IEEE 13-bus feeder topology [24] with the same modifications and assumptions as [7]. The pump is connected to bus 10. We set η_e to 3. The minimum and maximum voltage limits are 0.95 pu and 1.05 pu, respectively. The nominal power demands at each bus and phase are multiplied by 1.5 so that the PDN is heavily loaded and the voltages are close to their minimum voltage limit. The power demand forecast error is uncertain but bounded between $[-\sigma \bar{\rho}_{k,\phi}^t, \sigma \bar{\rho}_{k,\phi}^t]$ at each bus and phase with a load present, where σ indicates a percentage of the forecasted load. We set $\pi_e^t = \$100/\text{MWh}$ and $\pi_{vs,e}^t = \$10/\text{MWh}$. We solve the problem with the JuMP package in Julia using the SCIP [25] and Gurobi [26] solvers.

B. Results

We first evaluate the robust solutions for a single time period while varying the size of the uncertainty set (i.e., by varying σ). In Table I, we present the objective cost, the scheduled pump power consumption, and the full range of real-time pump power adjustments $R^t = R_{\rm up}^t + R_{\rm dn}^t$ for the robust voltage support problem with convex WDN

TABLE I SINGLE-PERIOD RESULTS

σ (%)	Objective Cost (\$)	Sched. Pump Power (kW)	R^t (kW)
2	67.16	671.61	0
3	68.79	671.61	162.90
4	71.87	671.61	470.58
5	74.94	671.61	778.20

constraints. For all cases in Table I, the scheduled pump power consumption is constant because the tank injections must be non-positive (12a) and the scheduled pump power consumption is minimized (i.e., the scheduled tank injection is zero). When $\sigma=2\%$, the PDN does not experience voltage limit violations for any realization of uncertain power demand. Therefore, the control policy is zero and the water pumps do not adjust their operation in real-time. As the power demand uncertainty increases, a non-zero control policy is needed to handle some of the uncertainty realizations. Consequently, the objective cost and R^t increase.

We check the robustness of the solutions in Table I with the original, nonconvex WDN constraints and the linearized PDN constraints. We randomly generated 1,000 uniformly distributed power demand forecast error scenarios within the uncertainty set. Given the scheduled pump power consumption and the parameters of the pump power control policy, we calculated the real-time pump power adjustments and verified that the power flow equations and the nonconvex water flow equations are satisfied. We found that the solutions are feasible in the robust nonconvex problem for all uncertainty scenarios tested.

Next, we solve the robust voltage support problem for a 24-hour period. In Fig. 4, we compare the solution of the robust problem to that of a deterministic problem that uses only the forecasted demands. We observe that the robust schedule (17a) varies less than the deterministic schedule. This is because the robust solution needs to be feasible for the entire range of pump power adjustments around the schedule, i.e., $-R_{\rm dn,e}^t$ and $+R_{\rm up,e}^t$. The range of pump power adjustments results in robust bounds around the WDN's adjustable variables (e.g., the pump flow rates and the tank levels). We illustrate the range of bounds for the extreme cases (17b)-(17c) in Fig. 4 with a blue shaded area.

The robust bounds of the tanks in Fig. 4 demonstrate the propagation of uncertainty over multiple time periods. In our formulation, the tank level (12b) is a function of the tank level in the previous time period. As a result, the tank's robust bounds are dependent on the uncertainty from previous time periods. As expected, the tank bounds increase over time due to propagation of uncertainty across time periods. We were unable to robustly solve the 24-hour problem for larger uncertainty levels (e.g. $\sigma = 5\%$), indicating that the solution becomes increasingly conservative as the uncertainty accumulates over the scheduling horizon until the robust problem becomes infeasible. There are methods to deal with uncertainty propagation, such as compensating for recently observed forecast error [27], but we leave this to future work.

Next, we verify the computational tractability of the robust voltage support problem by comparing the solver time of the

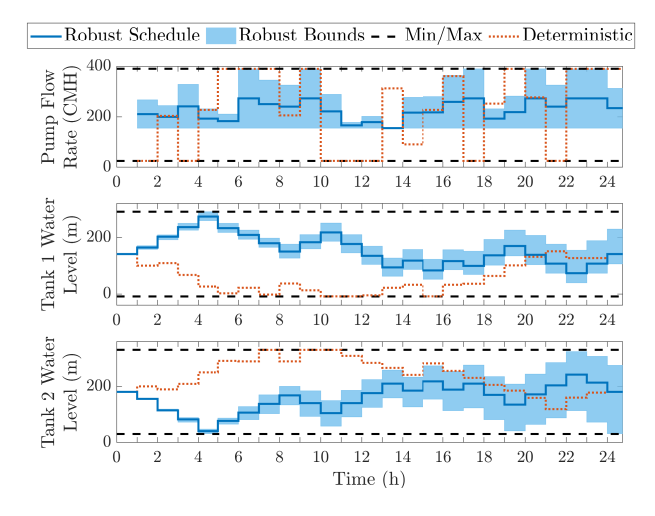


Fig. 4. Pump flow rates and tank levels in the multi-period convex robust problem ($\sigma=4\%$) for the robust schedule (solid blue lines) and the deterministic schedule based on forecasted demands (red dotted lines). The bounds on the robust pump flow rate and tank levels are shown with blue shading around the schedule. The black dashed lines are the minimum and maximum pump flow rates and tank levels.

robust problem with that of the chance-constrained voltage support formulation solved via the scenario approach in [28]. The results in [28] are generated using a comparably sized WDN. When solving the voltage support problem for 3 time periods, the robust problem's solver time was less than a second whereas the chance-constrained problem's solver time was 10-50 minutes. For a scheduling horizon of 24 hours, we were unable to solve the chance-constrained problem due to memory issues whereas solving the robust problem takes less than 2 seconds. This comparison demonstrates the computational tractability of our proposed formulation.

VI. CONCLUSION

In this paper, we formulated an ARO problem that controls water pumping in the WDN to provide voltage support to the PDN given power demand uncertainty. We apply the monotonicity properties from [2] to the WDN and identify the tank operation assumptions needed to ensure monotonicity. Using these properties, along with affine control policies and constraint approximations, we reformulated the problem as a tractable AARC. In our case study, we demonstrated the robustness and computational tractability of our approach. However, we found that the assumptions needed to enforce monotonicity significantly restrict the feasible water flow solutions. In the future, we will explore methods to reduce the propagation of uncertainty and incorporate booster pumps into the formulation.

REFERENCES

- P. Mancarella, G. Andersson, J. A. Peças-Lopes, and K. R. W. Bell, "Modelling of integrated multi-energy systems: drivers, requirements, and opportunities," *Proc. Power Syst. Comput. Conf. (PSCC)*, 2016.
- [2] M. Vuffray, S. Misra, and M. Chertkov, "Monotonicity of dissipative flow networks renders robust maximum profit problem tractable: General analysis and application to natural gas flows," in *Proc. IEEE* Conf. Decis. Control (CDC), 2015, pp. 4571–4578.
- [3] Q. Li, S. Yu, A. Al-Sumaiti, and K. Turitsyn, "Micro water-energy nexus: optimal demand-side management and quasi-convex hull relaxation," *IEEE Trans. Control Netw. Syst.*, 2018.

- [4] Y. Liu, C. Barrows, J. Macknick, and M. Mauter, "Optimization framework to assess the demand response capacity of a water distribution system," *J. Water Resour. Plan. Manag.*, vol. 146, no. 8, pp. 1–13, 2020.
- [5] K. Oikonomou and M. Parvania, "Optimal coordination of water distribution energy flexibility with power systems operation," *IEEE Trans. Smart Grid*, vol. 10, no. 1, pp. 1101–1110, 2019.
- [6] D. Fooladivanda, A. D. Dominguez-Garcia, and P. Sauer, "Utilization of water supply networks for harvesting renewable energy," *IEEE Trans. Control Netw. Syst.*, vol. 6, no. 2, pp. 763 – 774, 2019.
- [7] A. Stuhlmacher and J. L. Mathieu, "Chance-constrained water pumping to manage water and power demand uncertainty in distribution networks," *Proc. IEEE*, vol. 108, no. 9, pp. 1640–1655, 2020.
- [8] M. C. Campi, S. Garatti, and M. Prandini, "The scenario approach for systems and control design," *Annual Reviews in Control*, vol. 33, no. 2, pp. 149–157, 2009.
- [9] S. Misra, M. Vuffray, and A. Zlotnik, "Monotonicity properties of physical network flows and application to robust optimal allocation," *Proc. IEEE*, vol. 108, no. 9, pp. 1558–1579, 2020.
- [10] L. A. Roald, K. Sundar, A. Zlotnik, S. Misra, and G. Andersson, "An uncertainty management framework for integrated gas-electric energy systems," *Proc. IEEE*, vol. 108, no. 9, pp. 1518–1540, 2020.
- [11] D. Verleye and E.-H. Aghezzaf, "Optimising production and distribution operations in large water supply networks: A piecewise linear optimisation approach," *Int. J. Prod. Res*, vol. 51, no. 23-24, pp. 7170– 7189, 2013.
- [12] A. Ben-Tal, L. El Ghaoui, and A. Nemirovski, Robust optimization. Princeton University Press, 2009, vol. 28.
- [13] D. B. Arnold, M. Sankur, R. Dobbe, K. Brady, D. S. Callaway, and A. Von Meier, "Optimal dispatch of reactive power for voltage regulation and balancing in unbalanced distribution systems," *Proc.* IEEE Power Energy Soc. Gen. Meeting, 2016.
- [14] A. Bernstein, C. Wang, E. Dall'Anese, J. Le Boudec, and C. Zhao, "Load flow in multiphase distribution networks: Existence, uniqueness, non-singularity and linear models," *IEEE Trans. Power Syst.*, vol. 33, no. 6, pp. 5832–5843, Nov 2018.
- [15] J. Löfberg, "Automatic robust convex programming," Optimization methods and software, vol. 27, no. 1, pp. 115–129, 2012.
- [16] P. R. Bhave and R. Gupta, Analysis of water distribution networks. Oxford, U.K.: Alpha Science International Ltd., 2006.
- [17] M. K. Singh and V. Kekatos, "Optimal scheduling of water distribution systems," *IEEE Trans. Control Netw. Syst.*, vol. 7, no. 2, pp. 711–723, 2020.
- [18] J. Burgschweiger, B. Gnädig, and M. C. Steinbach, "Optimization models for operative planning in drinking water networks," *Optim. Eng.*, vol. 10, no. 1, pp. 43–73, 2009.
- [19] S. Pabi, A. Amarnath, R. Goldstein, and L. Reekie, "Electricity use and management in the municipal water supply and wastewater industries," Electric Power Research Institute, Tech. Rep. 3002001433, 2013.
- [20] K. E. Lansey and K. Awumah, "Optimal pump operations considering pump switches," J. Water Resour. Plan. Manag., vol. 120, no. 1, pp. 17–35, 1994.
- [21] M. K. Singh and V. Kekatos, "On the flow problem in water distribution networks: Uniqueness and solvers," *IEEE Trans. Control Netw.* Syst., vol. 8, no. 1, pp. 462–474, 2021.
- [22] E. Todini and S. Pilati, "A gradient method for the analysis of pipe networks," Proc. Computer Applications for Water Supply and Distribution, 1988.
- [23] OWA-EPA, "Epanet," http://github.com/OpenWaterAnalytics/EPANET,
- [24] W. H. Kersting, "Radial distribution test feeders," Proc. IEEE Power Eng. Soc. Winter Meeting, vol. 2, pp. 908–912, 2001.
- [25] G. Gamrath, D. Anderson, K. Bestuzheva, W.-K. Chen, L. Eifler, M. Gasse, P. Gemander, A. Gleixner, L. Gottwald, K. Halbig, et al., "The SCIP optimization suite 7.0," 2020.
- [26] Gurobi optimizer 8.1. [Online]. Available: http://www.gurobi.com
- [27] L. Herre, J. L. Mathieu, and L. Söder, "Impact of market timing on the profit of a risk-averse load aggregator," *IEEE Trans. Power Syst.*, vol. 35, no. 5, pp. 3970–3980, 2020.
- [28] A. Stuhlmacher and J. L. Mathieu, "Water distribution networks as flexible loads: a chance-constrained programming approach," Proc. Power Syst. Comput. Conf. (PSCC), 2020.